Catalytic decomposition of acetylene on Fe(001): A first-principles study

Gun-Do Lee,[1] Seungwu Han,[2] Jaejun Yu,[1,2] and Jisoon Ihm[1]

[1] *School of Physics, Seoul National University, Seoul 151-742, Korea*

[2] *Center for Strongly Correlated Materials Research, Seoul National University, Seoul 151-742, Korea*

The catalytic decomposition process in the initial stage of carbon nanotube (CNT) growth is investigated for the system of acetylene (C_2H_2) on the Fe(001) surface through first-principles electronic structure calculation. In its most stable configuration, the C-C bond of C_2H_2 is lying on the hollow site along the [110] direction of the Fe(001) surface. The formation of the CH fragments accompanied by C-C bond breaking is found to be an intermediate step toward the full dissociation of C_2H_2 molecules on Fe(001) and the whole process is exothermic.

Surface catalysis has been a long-standing issue in many areas of physics and chemistry. The oxidation of carbon monoxide on transition metal surfaces[1–3] is one of the most extensively studied heterogeneous catalytic reactions related to the air pollution problem. The dissociative interaction between methane and a metal surface[4,5] has also been studied as an example of activated adsorption. Relatively less attention was paid to the interaction between metal surfaces and simple hydrocarbons such as acetylene (C_2H_2) and ethylene (C_2H_4). Recently, as the growth technique of carbon nanotube (CNT) develops, the role of a metal catalyst for simple hydrocarbons has become an important issue in both physics and chemistry. The synthesis of the CNT has attracted a lot of interest because of its potential technological applications such as field emission displays,[6] hydrogen storage,[7] and chemical sensors.[8] To control the detailed characteristics of the CNT growth, it is required to understand the role of metal catalysts at a fundamental level. While the role of transition metal catalysts during the synthesis of the CNT has been studied by several groups, most studies have focused on the growth process itself where the metal is considered to catalyze the assembly of carbon hexagons from carbon feedstock diffusing along the nanotube wall.[9–11] In fact, another important role of the metal catalyst is the decomposition of hydrocarbons in the initial stage of the CNT growth, which is a crucial step in the growth process with the chemical vapor deposition (CVD) method. Not much theoretical understanding on the microscopic mechanism of such a catalytic decomposition process is available, especially with regard to the catalytic reaction of hydrocarbons on transition metal surfaces. Although several state-of-the-art electronic structure calculations for the catalytic reaction of simple molecules have been tried,[2–4] no first-principles approach has been taken for probing the full decomposition process of hydrocarbon molecules on the metal surfaces to our knowledge.

In this paper, we present the results of our first-principles calculations on the decomposition process of a hydrocarbon molecule on the Fe substrate. As a representative system, we consider acetylene (C_2H_2) on the Fe(001) surface, which is considered to be a basic model for the understanding of heterogeneous catalysts. The Fe substrate is known to be highly effective for the CNT growth with C_2H_2 in the CVD

process.[12] In this study, we predict the energy minimum configuration of C_2H_2 on Fe(001) and provide a comprehensive picture for the decomposition process of C_2H_2 on the metal surface through the analysis of energetics and bond configurations between carbon and metal atoms.

The calculation is carried out in the framework of the density functional theory by using the pseudopotential method[13] within the generalized gradient approximation (GGA) of the Perdew-Burke-Ernzerhof (PBE) form.[14] GGA is generally known to be better than local spin density approximation (LSDA) in describing structural and magnetic properties of Fe.[15] Vanderbilt ultrasoft pseudopotentials[16] are used with a 30 Ry energy cutoff. In generating the Fe pseudopotential, the semirelativistic effect is included and the exchange interaction with the core charge is taken into account through the partial core correction.[18] Pseudopotentials are checked carefully for bulk Fe and isolated C_2H_2 molecules.[17] The surface is simulated as a slab containing four layers of Fe. The 13.5-Å-thick vacuum is inserted between the repeated slabs. We take a 2×2 supercell in the lateral directions. Adsorbates are placed on both sides of the slab, maintaining the inversion symmetry of the system. Interactions between adsorbates in different supercells are found to be negligible. Nine **k** points are selected in the 3 $\times 3$ regular meshes (avoiding the Γ point) in the two-dimensional irreducible Brillouin zone. Structural relaxations are performed until the force on each atom is less than 0.05 eV/Å. In the calculation of dissociation barriers, the distance between two atoms under consideration for dissociation is systematically varied while all the rest of the atoms are allowed for full relaxations.

To find the minimum energy configuration of C_2H_2 on the surface, we calculate total energies for various configurations as shown in Fig. 1(a), especially along the pathway from the bridge site (the configuration BR) to the hollow site (the configuration H) of the Fe(001) surface. On the bridge site, we consider C_2H_2 lying along the [100] direction of the Fe substrate, which is energetically more stable than other orientations. For instance, C_2H_2 lying along the [100] direction of the bridge site is more stable than the one lying along the [010] direction by 0.62 eV in total energy per molecule. We also calculate total energies while rotating C_2H_2 from the configuration H to A [see Fig. 1(b)]. As a result, configura-
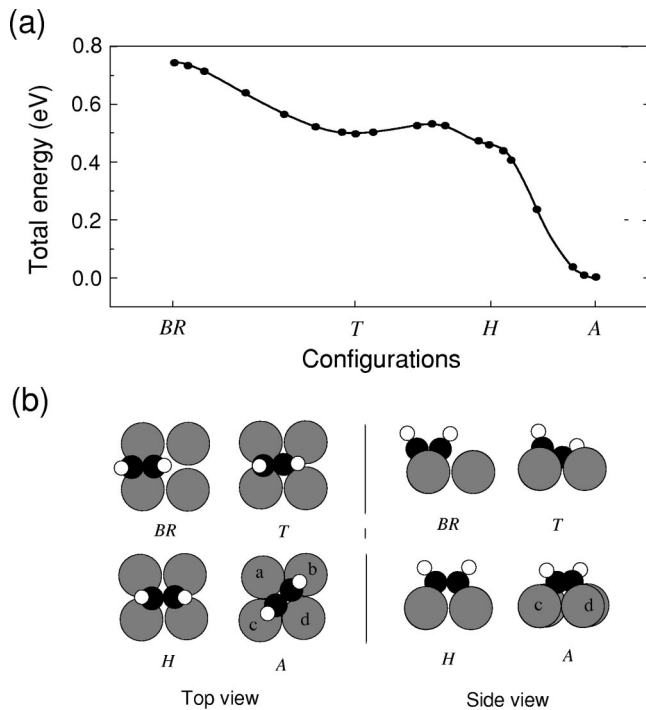
FIG. 1. (a) Total energy variation along the diffusion pathway of C_2H_2 on Fe(001), (b) the top views and side views of the configurations. Energies in (a) are plotted with respect to that of the configuration A. The reaction coordinate (the abscissa) in the interval (BR, H) of (a) is the position of the center of the C-C bond in the x direction, while that in the interval (H,A) is the rotation angle of the C-C bond. Black, white, and gray circles in (b) represent C, H, and Fe atoms, respectively.

tion A turns out to be the lowest in energy. This result is consistent with the experimental observation of the C_2H_2 molecular configuration on the Cu(001) surface.[19] In the minimum energy configuration A of C_2H_2 on Fe(001), the C-C bonds are rotated by 45° with respect to the [100] direction. The length of the C-C bond and the C-H bond is 1.39 Å and 1.11 Å, respectively. The bond length between a carbon atom and its neighboring Fe atom is 1.92 Å. The C-H bond is bent up to 59.6° with respect to the Fe surface. In the fully relaxed geometry of configuration A, it is interesting to note that the Fe-Fe distance along the C-C bonds [i.e., the distance between atom "b" and "c" in Fig. 1(b)] does not change appreciably, whereas the Fe-Fe distance across the C-C bonds [i.e., the distance between atom "a" and "d" in Fig. 1(b)] contracts significantly ($\sim 10\%$) relative to that of the clean Fe(001) surface.

In contrast to the previous result by molecular orbital analysis,[20] the configuration H is not an energy minimum (not even a local minimum) in our calculation. Instead, the configuration T is a shallow local minimum. The C-C bond of C_2H_2 in the configuration T is tilted by 22.2° relative to the surface plane and one of carbon atoms occupies the center of the hollow site. The energy of T is higher than that of A by 0.50 eV. The diffusion barrier (A to BR) of the C_2H_2 molecule in moving to the next hollow site is found to be 0.74 eV. Our GGA results for some principal geometries of C_2H_2 on Fe(001) was checked against the LSDA results.[21]
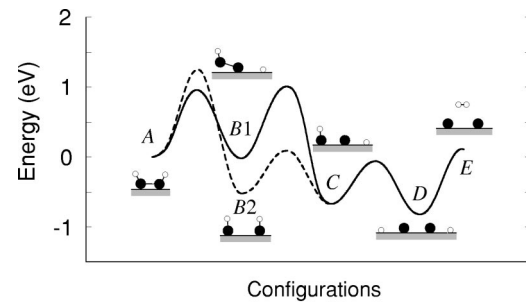

FIG. 2. Energy diagram for the process of the C_2H_2 decomposition. The solid line indicates the decomposition process following the A-$B1$-C-D-E sequence while the process involving $B2$ (instead of $B1$) is indicated by the dashed line. Atomic geometries are schematically drawn for local energy minima as well as both ends of the sequence. Black and white circles in the ball-and-stick model represent the C and H atoms, respectively, and the shaded plane represents the Fe substrate.

To investigate the decomposition process of C_2H_2 on Fe(001), we consider two possible pathways starting from the configuration A, i.e., the C-H bond breaking and the C-C bond breaking. These intermediate states are indicated as $B1$ and $B2$ in Fig. 2, respectively. First, we consider the dissociation of H atom from the C_2H_2 molecule. As illustrated in Fig. 2, the separated acetylide (CCH) and H reach the intermediate stage $B1$ and individual fragments occupy different hollow sites. Here the total energy of $B1$ is slightly lower (0.02 eV) than that of A. Along the pathway $A \rightarrow B1$, the calculated energy barrier for detaching H is 0.96 eV. For comparison, the dissociation energy of the first hydrogen atom from an isolated C_2H_2 molecule in vacuum is as large as 5.58 eV, which is too high for hydrogen atoms to be dissociated even in the temperature range (700°C–1000°C) of the CNT growth by the CVD method. Second, we can consider the pathway $A \rightarrow B2$ which is accompanied by the C-C bond breaking. In this case, the calculated energy barrier from A to $B2$ is 1.25 eV, which is higher than the energy barrier from A to $B1$. These results imply that the C-H bonds are easier to break than the C-C bonds for C_2H_2 on Fe(001). Owing to the lower energy barrier, CCH fragments may be observed more frequently than CH fragments in the first stage of the C_2H_2 decomposition on Fe(001). However, since the total energy of $B2$ is lower than that of $B1$ by 0.50 eV, both CCH and CH fragments may be observed experimentally.

There are still two possible ways in which the CCH in $B1$ is decomposed. One way is through the dissociation of H, and the other is via the C-C bond breaking. The energy barrier for the H dissociation is 1.54 eV, which is much greater than that (1.02 eV) for the C-C bond breaking. Further, the total energy of the C-C dimer with dissociated H (not shown in Fig. 2) is much higher than the CH fragment with an isolated C atom (the configuration C in Fig. 2). Therefore, from now on, we will only consider the configuration C. As illustrated in Fig. 2, the configuration C can be reached via another pathway from the configuration $B2$ through the decomposition of one of the two CH fragments. The energy barrier for the path $B2 \rightarrow C$ is determined to be 0.61 eV. The
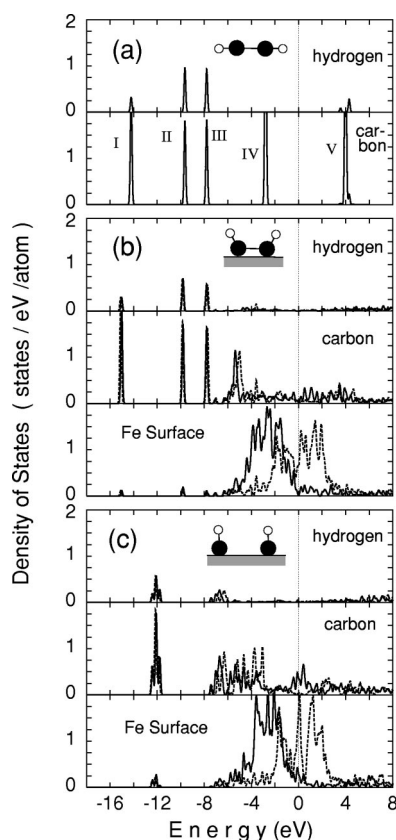
FIG. 3. PDOS of (a) an C_2H_2 molecule in vacuum, (b) C_2H_2 on the Fe(001) surface, and (c) the CH fragment on the Fe(001) surface. The solid and dotted lines indicate the DOS for spin-up and spin-down electrons, respectively.
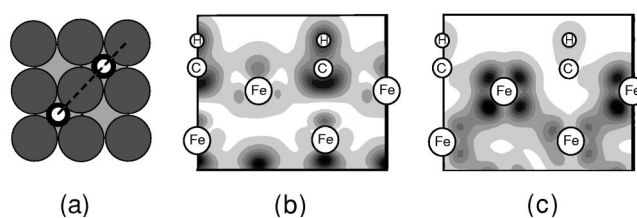

FIG. 4. (a) Top view of two CH fragments on Fe(001) and the charge density plots near the Fermi level for (b) the spin-up and (c) the spin-down states. Black, white, dark gray, and bright gray circles in (a) represent C, H, surface Fe atoms, and second layer Fe atoms, respectively. The charge density plots in (b) and (c) are drawn on the $(1\bar{1}0)$ plane as marked in dashed line in (a). Successive gray levels run from 0.0001 electrons/(a.u.)^3 in steps of 0.0002 electrons/(a.u.)^3.

configuration C is energetically more stable than $B2$. The existence of CH and CCH fragments during the decomposition process was observed in experiment.[22] The decomposition process after the stage C should be unique, namely, the dissociation of H from the remaining CH fragment to form the configuration D, where constituent atoms are fully separated on the Fe(001) surface. The energy barrier from C to D is also 0.61 eV and the total energy of D is lower than that of C by 0.15 eV. The total energy gain of D with respect to A is 0.82 eV per C_2H_2. In fact, the full dissociation is an exothermic process and the configuration D with isolated atoms are the most stable. In usual experimental situations, hydrogen atoms are expected to be desorbed in the form of molecule as indicated by E. As a result of the above reaction processes, isolated carbon atoms are expected to remain on Fe(001).[23] Our results show that the most stable position for the isolated carbon atom on Fe(001) is the fourfold hollow site.

To clarify the role of the Fe catalyst during the decomposition process, we have analyzed the electronic structures of C_2H_2 and the related CH fragments in detail. The projected density-of-states (PDOS) plots for an isolated C_2H_2 molecule, C_2H_2 on the Fe surface [corresponding to the configuration A in Fig. 1(b)], and CH fragments on the Fe surface ($B2$ in Fig. 2) are presented in Fig. 3. Three peaks labeled as I, II, and III in Fig. 3(a) originate from σ_s, σ_s^*, and σ_p bonding, respectively. The peak IV(V) corresponds to the

$pp\pi$ ($pp\pi^*$) state between two C atoms. Figure 3(b) is the PDOS plot of C_2H_2 adsorbed on the Fe surface in its minimum energy configuration A. The σ states (peaks I, II, and III) between C and H atoms are not much changed except for a small shift due to bending and stretching of the C-H bonds. On the other hand, because of the strong hybridization between the C $p\pi$ states and the Fe d orbitals, the characteristic $pp\pi$ bonding feature of C_2H_2 disappears and is changed into a broad spectrum covering the range of Fe d bands, which leads to the weakening of C-C bonding in comparison with that of isolated C_2H_2. The PDOS of CH fragments, as shown in Fig. 3(c), shows a distinct feature of the σ_s bond, which corresponds to the split peaks of σ_s and σ_s^* of the C_2H_2 with C-C bonds. Further, the trace of the σ_p bonding state and the broad $pp\pi$ feature in the PDOS of C_2H_2 on Fe(001) are absent in CH fragments on Fe(001). Instead, a rather broad spectrum corresponding to the hybridization of C p orbitals and Fe d band states appears in the case of CH fragments. In addition, it is observed that a strong peak at the Fermi level develops as a result of strong spin-dependent hybridization between the C $p\pi$ electrons and Fe d electrons related to the Fe surface state. Figure 4(b) and 4(c) show the spin-projected charge density plots of CH fragments on Fe(001) for the states near the Fermi level. In the spin-up channel, the C p states and Fe e_g states develop a strong bonding feature, whereas the spin-down component of the C p states and Fe t_{2g} states has the antibonding character. Indeed, the spin-dependent coupling for the CH fragments on Fe(001) seems to be more enhanced than the case of C_2H_2 on Fe(001). The changes in the number of major peaks near the Fermi level and their relative intensities would be useful information for the experimental confirmation of the dynamical process proposed here.

Our calculations demonstrate that carbon atoms distribute over the hollow sites on Fe(001) as a result of the C_2H_2 decomposition. This leads to the conjecture that carbon structures (nanotube, graphene sheet, cluster, etc.) growing on a metal surface might depend on the lattice matching condition with the substrate. For example, the periodicity of the graphite lattice is well matched with those of Rh(111) and Pt(111). On such metal surfaces, the grapheme sheet may preferentially be formed.[24] On the contrary, a large mismatch of the lattice periodicity between the graphite and the

hollow sites on Fe(001) will not favor the graphite structure. Therefore, as the number of accumulated carbon atoms on Fe(001) increases, they are expected to become connected and consequently develop defects such as pentagons or heptagons. This may promote the growth of CNT's by introducing a curvature into the graphite plane.

In summary, we have studied the detailed process of the C_2H_2 decomposition on the Fe(001) surface, which occurs in the initial stage of the CNT growth, through first-principles density functional calculations. We have found that the most stable configuration of the C_2H_2 molecule on Fe(001) is the configuration A as shown in Fig. 1 where the C-C bond of C_2H_2 is lying along the [110] direction on the hollow site. During the decomposition of C_2H_2, the strong hybridization between C and Fe atoms causes the weakening of the C-H and C-C bonds. The C-C bond breaking and the formation of the CH fragments have been found to precede the full dissociation of the constituent atoms of C_2H_2. The full dissociation into isolated atoms is also found to be the most favorable energetically and to be an exothermic process. Our results may also serve as a basis for the further study of the growth mechanism of the CNT as well as the catalytic decomposition of hydrocarbons on metal surfaces in general.

[1] C.C. Cudia, S.W. Hla, G. Comelli, Ž. Šljivančanin, B. Hammer, A. Baraldi, K.C. Prince, and R. Rosei, Phys. Rev. Lett. **87**, 196104 (2001)

[2] A. Alavi, P. Hu, T. Deutsch, P.L. Sivestrelli, and J. Hutter, Phys. Rev. Lett. **80**, 3650 (1998).

[3] C. Stampfl and M. Scheffler, Phys. Rev. Lett. **78**, 1500 (1997).

[4] G. Henkelman and H. Jónsson, Phys. Rev. Lett. **86**, 664 (2001).

[5] A.V. Walker and D.A. King, Phys. Rev. Lett. **82**, 5156 (1999).

[6] S. Fan, M.G. Chaline, N.R. Franklin, T.W. Tombler, A.M. Casell, and H. Dai, Science **283**, 512 (1999).

[7] A.C. Dillon, K.M. Jones, T.A. Bekkedahl, C.H. Kiang, D.S. Bethune, and M.J. Heben, Nature (London) **386**, 377 (1997).

[8] J. Kong, N.R. Franklin, C. Zhou, M.G. Chapline, S. Peng, K. Cho, and H. Dai, Science **287**, 622 (2000).

[9] A.N. Andriotis, M. Menon, and G. Froudakis, Phys. Rev. Lett. **85**, 3193 (2000).

[10] Y.H. Lee, S.G. Kim, and D. Tomanek, Phys. Rev. Lett. **78**, 2393 (1997).

[11] J. -C. Charlier, A. De Vita, X. Blase, and R. Car (unpublished).

[12] A. Fonesca, K. Hernandi, P. Piedigrosso, J.-F. Colomer, K. Mukhopadhyay, R. Doome, S. Lazarescu, L.P. Biro, Ph. Lambin, P.A. Thiry, D. Bernaerts, and J.B. Nagy, Appl. Phys. A: Mater. Sci. Process. **67**, 11 (1998).

[13] J. Ihm, A. Zunger, and M.L. Cohen, J. Phys. C **12**, 4409 (1979).

[14] J.P. Perdew, K. Burke, and M. Ernzerhof, Phys. Rev. Lett. **77**, 3865 (1996)

[15] E.G. Moroni, G. Kresse, J. Hafner, and J. Furthmuller, Phys. Rev. B **56**, 15 629 (1997)

[16] D. Vanderbilt, Phys. Rev. B **41**, 7892 (1990).

[17] For example, for the bcc Fe bulk, the calculated lattice constant is 2. 847 (2. 867) Å, bulk modulus is 1. 687 (1. 683) Mbars, and magnetic moment is 2.31 μ_B (2.22 μ_B). Experimental values in parentheses are quoted from C. Kittel, *Introduction to Solid State Physics*, 7th ed. (Wiley, New York, 1996). The lengths of the C-C bond and the C-H bond in isolated C_2H_2 molecules are 1. 204 (1. 20) Å and 1. 068 (1. 06) Å, respectively. Experimental values in parentheses are quoted from J. McMurry, *Organic Chemistry* (Brooks/Core, Belmont, MA, 1996).

[18] S.G. Louie, S. Froyen, and M.L. Cohen, Phys. Rev. B **26**, 1738 (1982).

[19] B.C. Stipe, M.A. Rezaei, and W. Ho, Science **280**, 1732 (1998).

[20] A.B. Anderson and S.P. Mehandru, Surf. Sci. **136**, 398 (1984).

[21] In LSDA, the energy of the configuration T is slightly higher (0. 02 eV) than that of A, and the configuration H is found to be at the local energy minimum having a higher energy than A by 0. 36 eV.

[22] W.-H. Hung and S.L. Bernasek, Surf. Sci. **339**, 272 (1995).

[23] The total energy of two separated carbon atoms on different hollow sites is found to be lower by 1.15 eV than that of a carbon dimer on the hollow site, further confirming the existence of carbon as isolated atoms after the decomposition of C_2H_2 on Fe(001).

[24] B.E. Bent, C.M. Mate, J.E. Crowell, B.E. Koel, and G.A. Somorjay, J. Phys. Chem. **91**, 1493 (1987)

[25] S. Baroni, A. Dal Corso, S. de Gironcoli, and P. Giannozzi, http://www.pwscf.org .